Available online at www.sciencedirect.com

ScienceDirect

Proceedings of the Combustion Institute xxx (2014) xxx–xxx

Proceedings of the Combustion Institute

www.elsevier.com/locate/proci

Experimental study of the effect of CF_3I addition on the ignition delay time and laminar flame speed of methane, ethylene, and propane

O. Mathieu [a,*], J. Goulier [b], F. Gourmel [b], M.S. Mannan [c], N. Chaumeix [b], E.L. Petersen [a]

[a] Department of Mechanical Engineering, Texas A&M University, College Station, TX 77843, USA
[b] Institut de Combustion, Aérothermique, Réactivité et Environnement (ICARE) CNRS-INSIS 1C, avenue de la Recherche Scientifique, F-45071 Orléans Cedex 02, France
[c] Mary Kay O'Connor Process Safety Center, Artie McFerrin Department of Chemical Engineering, Texas A&M University, College Station, TX 77843, USA

Abstract

Since no suitable replacement has been found for Halon 1301 (CF_3Br), the approach for the next generation of fire suppressants has been to identify diverse agents or blends of agents for specific applications. Halon 13001 (CF_3I) is a possible candidate for unoccupied areas. However, there are very few fundamental data to help in validating its detailed kinetics mechanism. In this study, ignition delay time and laminar flame speed measurements of the effects of CF_3I on CH_4, C_2H_4, and C_3H_8 have been investigated for the first time. The ignition delay times were obtained in a shock tube with mixtures of fuel/O_2/CF_3I highly diluted in 98% argon (vol.), and the flame speeds were measured using an expanding, spherical flame. Results from the new experiments show a significant decrease in the laminar flame speed for small additions of suppressant. The effects on the ignition delay time are strongly dependent on the hydrocarbon: the ignition delay time of CH_4 is significantly decreased by CF_3I addition, while a significant increase in the ignition delay time was observed for the lowest temperatures investigated with C_2H_4. Ignition delay times for C_3H_8 were mostly unchanged, except for the lowest temperatures (below 1400 K) where a small decrease in the reactivity was observed. Compared to recent results obtained with CF_3Br, CF_3I showed a smaller suppressant effect under the conditions investigated. A detailed kinetics mechanism assembled from a C1–C3 mechanism from NUI Galway and a CF_3I sub-mechanism from NIST predicts well the results obtained in the shock tube with CH_4 and C_3H_8. The C_2H_4 data with CF_3I are however poorly predicted, pointing at some deficiencies in the model for C_2H_4/CF_3I interactions.

Keywords: Halon 13001; Ignition delay time; Laminar flame speed; Kinetic

* Corresponding author. Fax: +1 (979) 845 3081.
E-mail address: olivier.mathieu@tamu.edu (O. Mathieu).

http://dx.doi.org/10.1016/j.proci.2014.05.096
1540-7489/

1. Introduction

With its high suppression efficiency [1], along with a relatively low toxicity, Halon 1301 (CF_3Br) was the most commonly used fire suppressant prior to being phased-out by the Montreal Protocol. Although a large body of work has been performed to find a suitable replacement [2], no component that meets all the required criteria has been found [3]. To date, CF_3Br is still the subject of extensive research in order to have a detailed understanding of its combustion chemistry (to identify/design similar reaction pathways for candidate replacements) [4,5] and to serve as a benchmark for new compounds [3,6,7]. However, few – if any – fundamental combustion data have been available for the development of the CF_3Br chemical kinetics mechanism [1,8,9], explaining the discrepancy between the model and recent fundamental combustion data (ignition delay time (τ_{ign}) and laminar flame speed (S_L^0)) [5].

Since no single substitute for Halon 1301 has been found, a more likely approach is to identify diverse agents or blends of agents for specific applications. Amongst the possible replacement candidates, CF_3I (Halon 13001) displayed some interesting properties. Notably, when released into the lower atmosphere, the fluorinated iodoalkanes degrade by photolysis of the carbon–iodine bond and are expected to have short atmospheric lifetimes (and hence not reaching and depleting the ozone layer) [2]. Numerical studies have shown that it has the same extinction efficiencies, sometimes even superior on a molar basis, than CF_3Br for inhibiting CH_4, CH_3OH, C_2H_6, and C_2H_4 [10] and alkanes (C1–C4) burning velocities [6]. Smith and Everest [11] compared OH and soot concentration measurements in propane/air diffusion flames inhibited by CF_3Br or CF_3I. Overall, under their experimental conditions, CF_3I was slightly superior to CF_3Br in terms of (i) requiring smaller concentrations at extinction, and (ii) producing less within-flame soot. The reductions in the OH concentration were essentially the same for CF_3I and CF_3Br. The flame structure was compared between low-pressure flames doped with CF_3I or CF_3Br by Sanogo et al. [12]. Results showed that the flames are essentially similar, and species involved in the inhibition process are formed in similar amounts. CF_3I also has a boiling point that is low enough for in-flight application consideration, even if its release at high altitude can be problematic for the ozone layer [2]. One can however mention a few drawbacks with the use of CF_3I such as its cardiac sensitization at levels well below the extinguishing concentration, which restricts its utilization to unoccupied areas [2].

Despite the interesting characteristics of CF_3I, there is a noticeable lack of fundamental data to have a good understanding of its flame inhibition mechanisms and to better assess its fire suppressant potential. The aim of the present work was therefore to provide fundamental combustion data, namely ignition delay times (for kinetics model assessment) and laminar flame speeds (suppressant assessment), on the effects of CF_3I on methane (main component of natural gas), ethylene (one of the most-used hydrocarbons in the petrochemical industry), and propane (to represent saturated-chain hydrocarbons). Pressure conditions were the same as in Osorio et al. [5], but sub-atmospheric experiments were investigated as well herein using the shock-tube technique to account for possible in-flight applications.

2. Experimental set-up

2.1. Shock-tube

Ignition delay times were determined behind reflected shock waves (RSW) in a single-diaphragm, stainless-steel shock tube. The driven section is 15.24-cm i.d., 4.72-m long; and the driver section is 7.62-cm i.d., 2.46-m long. A schematic of the shock-tube setup can be found in Aul et al. [13]. Five PCB P113A piezoelectric pressure transducers, equally spaced alongside the driven section and mounted flush with the inner surface, were used to measure the incident-wave velocities. A curve fit of these four velocities was then used to determine the incident wave speed at the endwall location. Post reflected-shock conditions were obtained using this extrapolated wave speed in conjunction with the one-dimensional shock relations and the initial conditions. This method was proven to maintain the uncertainty in the temperature determination behind reflected shock waves below 10 K [14]. Test pressure was monitored by both a PCB 134A and Kistler 603 B1 transducers, located at, respectively, the endwall and sidewall (16 mm from the endwall) positions. Non-ideal boundary layer effects measured by the change in pressure (dP/dt) behind RSW were determined to be less than 2%/ms for all experiments. The corresponding increase in temperature for these dP/dt levels does not have a noticeable impact on the results herein, as we have shown in many other studies using this facility [5,13].

Experiments were performed at two different pressure conditions, around 0.9 and 1.7 atm, and three equivalence ratios (ϕ), 0.5, 1.0, and 2.0 for each mixture (neat hydrocarbon and hydrocarbon with 10% of the fuel molar percentage as CF_3I). Polycarbonate diaphragms were used (0.125 and 0.25 mm for the 0.9 and 1.7 atm experiments, respectively), and a cross-shaped cutter was employed to facilitate their breakage and prevent fragments from tearing off. Helium was used as the driver gas during this study.

Please cite this article in press as: O. Mathieu et al., *Proc. Combust. Inst.* (2014), http://dx.doi.org/10.1016/j.proci.2014.05.096

The driven section was vacuumed down to 2×10^{-5} Torr or better prior to every run. The pumping time between experiments was minimized using a pneumatically driven poppet valve matching the inside diameter of the driven section and allowing for a passage of 7.62-cm diameter between the vacuum section and the driven tube. Test mixtures were prepared manometrically in a stainless steel mixing tank. The mixing tank can be pumped down to pressures below 1×10^{-6} Torr. The gases (methane (99.97%), ethylene (99.995%), O_2 (99.999%) (Praxair), propane (Gas Innovation, 99.5%), Ar (AOC, 99.999%) and CF_3I (Alfa Aesar, 99.9%)) were passed through a perforated tube traversing the center of the mixing vessel to allow for rapid, turbulent mixing. Conditions investigated during this study are provided in Table 1, and the experimental results (τ_{ign} and corresponding pressure and temperature conditions behind the RSW) are provided as Supplementary material.

2.2. Spherical bomb

The bomb is a double-wall stainless-steel sphere (i.d. 476-mm) equipped with two opposite windows (100-mm diameter, 30-mm thick); with a black, polished inner surface. A thermal fluid flows between the walls for temperature homogeneity (measured at the inner side by a thermocouple (0.1 K precision)). Ignition was initiated at the center of the sphere by two metallic electrodes linked to a high-voltage source. The energy delivered by the spark (10 mJ maximum) was monitored using high-voltage and current probes. The pressure variation due to combustion is monitored via a piezoelectric pressure transducer (Kistler) mounted flush with the inner surface. The visualization of the flame is obtained via a schlieren system. A digital, high-speed camera (PHANTOM V1610) is used to record the schlieren images of the growing flames. These images allow the measurement of the flame radius as a function of time using a homemade, automatic MATLAB® program. Some sample images of spherical flames and evolution of the flame radius with time are available as Supplementary material. Depending on the equivalence ratio and to minimize the final error on the flame speed, between 400 and 700 images were recorded with a resolution of 0.13 mm/pixel at a framing rate of 25,000 frames/s. To correlate the pressure increase with the fast imaging, the image sampling and the pressure monitoring were synchronized using a TTL signal generated at the onset of the spark between the electrodes. This synchronization was mandatory to verify that the pressure did not deviate from its initial value during the observation time. When the flame radius reaches the radius of the window, only 0.8% of the total volume is burnt. More details on the apparatus can be found in Dubois et al. [15].

The combustible mixtures were prepared directly in the vessel using the partial pressure method. To have good precision on the equivalence ratio of the mixture (±0.2%), the partial pressure was monitored using two, high-sensitivity pressure gages (MKS-Baratron) with two different scales (0.133 and 133 kPa). Chemicals used during this study were CF_3I (Alfa Aesar, 97+%), methane, ethane, and propane grade N35 (Air Liquide). To remove any uncertainty on the air composition, Alpha-Gas-2 grade air with a molar composition of 20.9% O_2/0.791% N_2 was used.

Table 1
Composition of the mixtures investigated in the shock tube.

Fuel	ϕ	CF_3I (%)	Fuel (%)	O_2 (%)	Ar (%)
CH_4	0.5	0	0.4	1.6	98.0
		0.04	0.4	1.6	97.96
	1.0	0	0.667	1.333	98.0
		0.0667	0.667	1.333	97.9333
	2.0	0	1.0	1.0	98.0
		0.1	1.0	1.0	97.9
C_2H_4	0.5	0	0.286	1.714	98.0
		0.0286	0.286	1.714	97.9714
	1.0	0	0.5	1.5	98.0
		0.05	0.5	1.5	97.95
	2.0	0	0.8	1.2	98.0
		0.08	0.8	1.2	97.92
C_3H_8	0.5	0	0.182	1.818	98.0
		0.0182	0.182	1.818	97.9818
	1.0	0	0.333	1.667	98.0
		0.0333	0.333	1.667	97.9667
	2.0	0	0.571	1.1429	98.0
		0.0571	0.571	1.1429	97.9429

Please cite this article in press as: O. Mathieu et al., *Proc. Combust. Inst.* (2014), http://dx.doi.org/10.1016/j.proci.2014.05.096

The stoichiometry has been defined with the species CO_2, H_2O, HF, HI, and N_2 as the final products.

3. Experimental results

3.1. Shock tube

The ignition delay time was defined as the time between the passage of the RSW and the intersection of lines drawn along the steepest rate-of-change of OH• de-excitation (i.e., chemiluminescence) and a horizontal line which defines the zero-concentration level, as documented in Osorio et al. [5]. The chemiluminescence emission from the $A^2\sum^+ \rightarrow X^2\Pi$ transition of the excited-state hydroxyl radical (OH•) was followed at the sidewall location using an interference filter centered at 307 ± 10 nm with a Hamamatsu 1P21 photomultiplier tube in a custom-made housing.

Uncertainties in τ_{ign} are primarily due to the uncertainty in T_5 determination (below 10 K, as discussed above). As a result, the uncertainty in τ_{ign} reported in this study is around 10%. This uncertainty level takes into account the non-ideal boundary layer effects measured by the change in pressure (dP/dt) behind reflected shock waves. Some representative OH• and pressure profiles are provided as Supplementary material.

Ignition delay time measurements at around 1.7 atm for the (a) CH_4, (b) C_2H_4, and (c) C_3H_8 mixtures, both neat and doped with CF_3I, are visible in Fig. 1. For the three hydrocarbons, with and without fire suppressant, the ignition delay time increases with the equivalence ratio. However, the amplitude of the equivalence ratio effect depends on the hydrocarbon: a factor of 3 (low temperatures) to almost 4 (high temperatures) was observed between $\phi = 0.5$ and 2.0, respectively, for C_3H_8, whereas a factor of only 1.4 (high temperatures) to 1.8 (low temperatures) was observed with CH_4. The effects of the CF_3I addition also vary between each hydrocarbon: a noticeable decrease in τ_{ign} was observed with CH_4 when CF_3I was added to the mixture (Fig. 1(a)). This decrease in the ignition delay time is strongly dependent on the equivalence ratio: factors from 1.2 to 1.4 at $\phi = 2.0$; 1.6 to 1.75 at $\phi = 1.0$; and 1.7 to 2 at $\phi = 0.5$ were observed. For a fuel with a longer saturated chain like C_3H_8, Fig. 1(c), the ignition delay times are not changed by the CF_3I addition, except for the low-temperature extremities where increases in the ignition delay time are visible. Similar behavior is observed with C_2H_4 (Fig. 1(b)) but with increases in τ_{ign} significantly larger (by factors up to 2.4, 3.5, and 4.7 between the neat and doped mixtures at the lowest temperature for $\phi = 0.5$, 1.0, and 2.0, respectively). The increase in the ignition delay time also covers a larger range of temperature, which increases with the equivalence ratio. For the fuel rich case, an increase in τ_{ign} was observed over the entire range of temperatures investigated.

These behaviors linked to the change in the equivalence ratio are very similar for the other pressure investigated in this study, 0.9 atm. Data at this lower pressure are therefore not presented here but are visible in the Supplementary material section.

The effect of pressure on τ_{ign} is visible in Fig. 2 for the stoichiometric condition with (a) CH_4, (b) C_2H_4, and (c) C_3H_8. For the neat hydrocarbons, the increase in pressure reduces the ignition delay time. This reduction is however stronger for methane than for ethylene or propane. The fire suppressant effect also seems to be dependent on the pressure. The increase in τ_{ign} observed with propane when CF_3I was added is indeed larger at 0.9 atm than at 1.7 atm. The effect of Halon 13001 is however larger at the highest pressure with C_2H_4, especially on the low-temperature side.

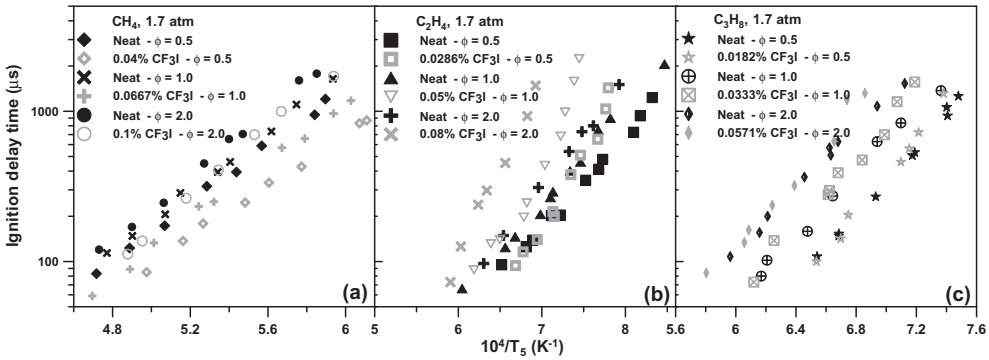

Fig. 1. Comparison between the ignition delay times of a neat-fuel mixture and the same mixture with 10% of the hydrocarbon replaced by CF_3I for (a) CH_4, (b) C_2H_4, and (c) C_3H_8 around 1.7 atm.

Please cite this article in press as: O. Mathieu et al., *Proc. Combust. Inst.* (2014), http://dx.doi.org/10.1016/j.proci.2014.05.096

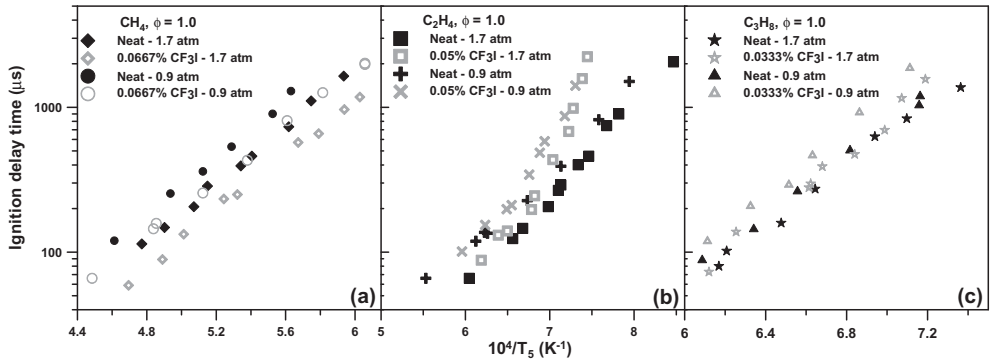

Fig. 2. Evolution of the ignition delay time with temperature for stoichiometric mixtures of (a) CH_4, (b) C_2H_4, and (c) C_3H_8 at 0.9 and 1.7 atm and with and without CF_3I.

With regard to methane, the decrease in the ignition delay time when the suppressant is added is the same over the entire range of temperatures and does not vary much with the pressure; reductions by a factor of around 1.5 were observed for the 0.9-atm case and around 1.7 for the higher-pressure condition.

3.2. Laminar flame speed

In this study, the laminar flame speed (S_L^0) was measured in the expanding flame configuration. Hence, the flame was subjected to stretch due to both curvature and strain. The total stretch rate at which a flame is submitted can be easily estimated by $\kappa = 2v_s/R_f$ with R_f the flame radius and $v_s = dR_f/dt$ the burning speed. When the stretch rate is low compared to the extinction limit, the flame speed varies non-linearly with κ following the analysis by Ronney and Sivashinsky [16]. In this case, the unstretched laminar flame speed v_s^0 is linked to v_s: $(v_s/v_s^0)^2 ln(v_s/v_s^0)^2 = -2L_b\kappa/v_s^0$. An example is given in Supplementary material. An unstretched laminar flame speed S_L^0 is deduced from the ratio between v_s^0 and the unburnt to the burn density ratio ($\sigma = \rho_u/\rho_b$). The density ratio was calculated herein using the equilibrium application of the COSILAB software [17].

To investigate the effect of CF_3I on S_L^0, 5% of the fuel was replaced by the suppressant. The stoichiometric coefficients for each mixture were calculated assuming that the combustion of the {0.95 CxHy + 0.05 CF_3I} mixture forms HF, HI, CO_2 and H_2O, as mentioned above. For one mole of fuel, 9.09 mol of air in the case of {0.95 CH_4 + 0.05 CF_3I}, 13.64 of air for {0.95 C_2H_4 + 0.05 CF_3I}, and 18.18 moles of air for {0.95 C_3H_8 + 0.05 CF_3I} are needed at $\phi = 1.0$.

Great care was taken to minimize the errors in the flame speed measurements. The high number of recorded images and the relatively large radius of the flame that can be used in the data processing lead to an error on the flame speed that was estimated to be at a maximum around ±1 cm/s. Laminar flame speeds of methane, ethylene, and propane mixtures in air were measured at an initial pressure of 1 atm for methane and of 1 bar for ethylene and propane. The initial temperature was 303 K, and a wide range of equivalence ratios was covered: $0.754 < \phi < 1.35$ for methane, $0.6 < \phi < 1.8$ for ethylene, and $0.7 < \phi < 1.152$ for propane.

Figure 3 illustrates the dependence on equivalence ratio of S_L^0 for (a) CH_4, (b) C_2H_4, and (c) C_3H_8 (c) mixtures. The maximum S_L^0 were found

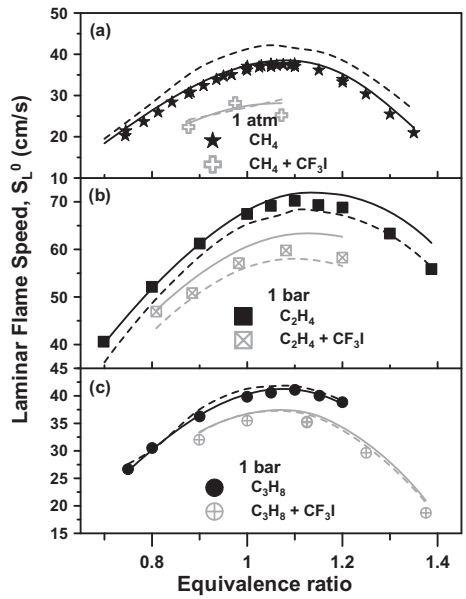

Fig. 3. Evolution of the laminar flame speed with equivalence ratio for (a) methane, (b) ethylene, and (c) propane. Closed symbols: without fire suppressant, open symbols: with 5% of CF_3I. All tests were performed at 303 ± 1 K. Lines: model [9,18]; dashed lines: model from NIST [9].

to be 37.5 cm/s for $\phi = 1.075$ with methane, 70.2 cm/s for $\phi = 1.1$ with ethylene, and 41.1 cm/s for $\phi = 1.1$ with propane. The substitution of methane by 5% of CF_3I induced a strong decrease in S_L^0: it diminished from 30.5 to 22.5 cm/s at $\phi = 0.88$ (20% decrease), from 35.2 to 28.2 cm/s at $\phi = 0.97$ (26% decrease) and from 37.5 to 25.2 cm/s at $\phi = 1.07$ (33% decrease) (Fig. 3a). The greater efficiency of CF_3I in reducing S_L^0 for ϕ ranging from 1 to 1.2 is even more visible in the cases of ethylene (Fig. 3b) and propane (Fig. 3c). The maximum laminar flame speed decreased from 70 to 60 cm/s for ethylene and from 40 to around 35 cm/s for propane.

3.3. Comparison with literature data

By comparing the data obtained in this study with the data obtained under similar conditions by Osorio et al. [5] with CF_3Br, Fig. 4, it is possible to compare the effects of the two fire suppressants on (a) CH_4 and (b) C_3H_8. At stoichiometric conditions, it is visible that CF_3Br and CF_3I have comparable effects on methane, the decrease in the ignition delay time being slightly higher at low temperature for CF_3I. For the propane case, a decrease in the ignition delay time is visible only at low temperatures with a CF_3I addition whereas the increase in τ_{ign} is larger and covers the entire range of temperature with CF_3Br. Other conditions ($\phi = 0.5$ and 2.0), for which trends are similar, are visible in the Supplementary material section.

The effect of CF_3I and CF_3Br can also be compared for methane laminar flame speed. Indeed, although the fire suppressant method was different between the two studies (5% of the fuel concentration in this study and 0.5% of the total mixture in Osorio et al. [5] for CF_3Br), their concentration is actually close around the stoichiometric condition. As can be seen in Fig. 5 for ϕ around 1.0 and 1.1, the suppressant effect is greater for CF_3Br than for CF_3I. Above $\phi = 1.1$, the concentration in CF_3I would be larger than the concentration of CF_3Br, so it is not possible to extrapolate the experimental trend to larger equivalence ratios.

Results of this study obtained for the neat hydrocarbon mixtures can also be compared with literature data. However, since the detailed study of τ_{ign} and S_L^0 for the neat hydrocarbon mixtures is beyond the scope of this work, figures for this comparison are visible in the Supplementary material section. Nevertheless, it can be mentioned that data from this study compare very well with the literature, especially given the variety of the configurations used in the literature data for S_L^0.

3.4. Model comparison

The data from the present study have been compared with the model from Babushok et al. [9]. Figure 6 shows the results of this comparison at stoichiometric conditions and at a pressure of 1.7 atm for (a) methane, (b) ethylene, and (c) propane, with and without CF_3I. Results show that the mechanism of Babushok et al. does not represent correctly the data for the neat CH_4 mixture, whereas the data for C_2H_4 and C_3H_8 are fairly well reproduced. The effects of the addition of CF_3I are well predicted for propane, and the decrease in the ignition delay time observed with methane is reproduced as well. However, the low-temperature increase in τ_{ign} with the suppressant addition to C_2H_4 is not captured. The CF_3I sub-mechanism from Babushok et al. [9] was then merged with the recent base hydrocarbon mechanism from Metcalfe et al. [18]. As can be seen in

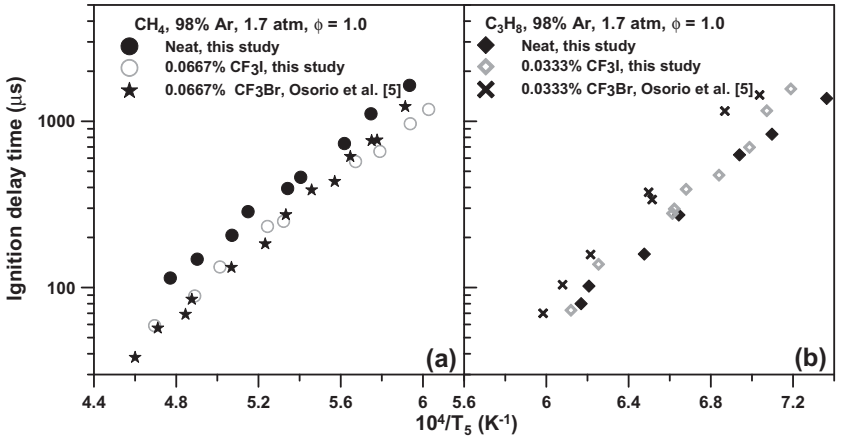

Fig. 4. Comparison between the effects of CF_3I from the present study and CF_3Br from Osorio et al. [5] on the ignition delay times of (a) CH_4 and (b) C_3H_8 at $\phi = 1.0$ and 1.7 atm.

Please cite this article in press as: O. Mathieu et al., *Proc. Combust. Inst.* (2014), http://dx.doi.org/10.1016/j.proci.2014.05.096

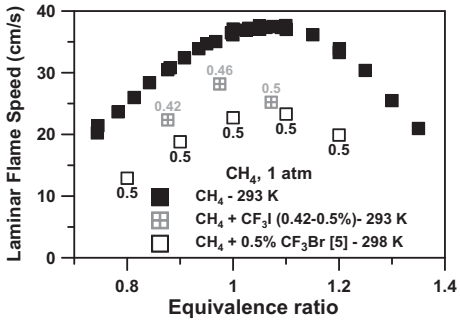

Fig. 5. Comparison between the effects of CF_3I and CF_3Br from Osorio et al. [5] on the laminar flame speed of CH_4. The numbers associated with the points in the figure refer to the fire suppressant percent in the mixture.

Fig. 5, all the neat fuel data are well predicted with this model. The data with CF_3I are also well predicted for CH_4 and C_3H_8, so results from the present study indicate that the CF_3I sub-mechanism needs improvement at the level of the interactions between CF_3I and C_2H_4.

The results of these comparisons between models and experiments shown above are representative of the other pressures and equivalence ratios investigated. The comparisons for the other conditions are therefore visible in the Supplementary material section.

The mechanisms were also used to model the laminar flame speed data. As visible in Fig. 3, the neat hydrocarbon data are better predicted by the model from Metcalfe et al. [18]. However, when this mechanism is merged with the CF_3I part from NIST [9], except for CH_4, the computed results are not as close to the experimental data as seen for the NIST model [9]. The current model also seems to poorly predict the CH_4/CF_3I flame speed results at both fuel rich and fuel lean conditions.

4. Discussion

During this study, the effect of CF_3I addition on the ignition delay times and laminar flame speeds of methane, ethylene, and propane were investigated experimentally. The addition of CF_3I was found to decrease τ_{ign} for methane. A similar effect was observed with CF_3Br over similar conditions by Osorio et al. [5]. A sensitivity analysis points at the same reaction for the two suppressants: $CF_3 + O_2 \rightleftarrows CF_3O + O$ (r1).

For C_3H_8, no reaction involving CF_3I or its products is amongst the 25 most-sensitive reactions at high temperature, explaining the lack of effect of CF_3I on C_3H_8 at this condition and on the ability of the current mechanism to reproduce this behavior. At the lower temperatures investigated, three reactions linked to the suppressant are inhibiting the reactivity of the τ_{ign} data: $CH_3I + M \rightleftarrows CH_3 + I + M$ (r2), $H + CH_3I \rightleftarrows HI + CH_3$ (r3) and $I + HO_2 \rightleftarrows HI + O_2$ (r4). The inhibiting effect is due to r3 that changes a reactive radical H into a less-reactive radical CH_3, with CH_3I being formed through r2. Another important fraction of the radical I is consumed via the terminating reaction r4, which also decreases the reactivity. The last two reactions are part of a larger catalytic mechanism, described below, which explains the inhibiting activity of CF_3I.

The comparison between the effects of CF_3I and CF_3Br on the ignition delay time showed that CF_3Br is overall slightly more reactive than CF_3I under the present conditions. However, according to Babushok et al. [9], CF_3I is able to inhibit the ignition at temperatures lower than for CF_3Br. This higher activity of CF_3I at low temperatures was confirmed in the present study for the lowest temperatures investigated with CH_4 and C_3H_8, as visible in Fig. 4.

The inhibiting effect of CF_3I for light hydrocarbon flames was detailed by Noto et al. [1].

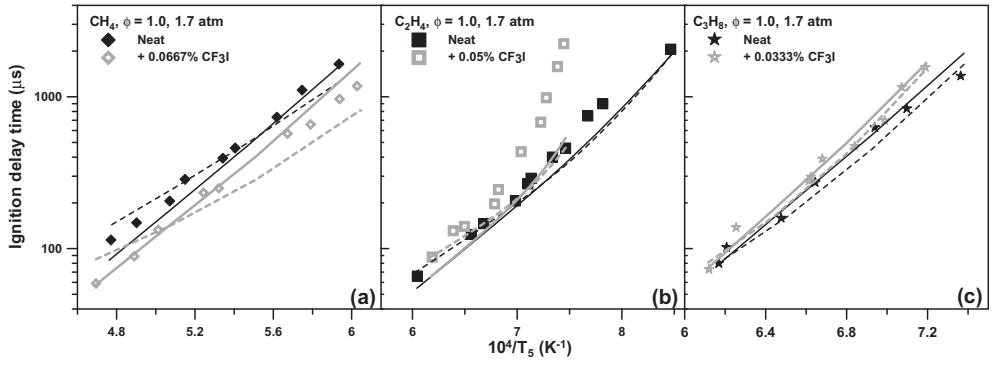

Fig. 6. Comparison between experimental data and models at $\phi = 1.0$ and around 1.7 atm for (a) CH_4, (b) C_2H_4, and (c) C_3H_8. Continuous lines are for the model from Metcalfe et al. [18] merged with the CF_3I sub-mechanism from Babushok et al. [9]; dashed lines correspond to the model from Babushok et al. [9]; the color black refers to the neat data, while grey corresponds to the data with CF_3I.

Please cite this article in press as: O. Mathieu et al., *Proc. Combust. Inst.* (2014), http://dx.doi.org/10.1016/j.proci.2014.05.096

Two mechanism pathways are involved: the first mechanism, common to both CF_3Br and CF_3I, involves the fluorinated part of these molecules. The CF_3 radical is involved in scavenging reactions such as $CF_3 + H \rightleftarrows CF_2 + HF$ and $CF_3 + CH_3 \rightleftarrows HF + CH_2{:}CF_2$ which reduce the reactivity of the mixture. However, most of the suppressant effect comes from the iodine part, which is involved in a catalytic cycle that transforms important radicals into stable products as shown below.

HI formation:

$$I + HO_2 \rightleftarrows HI + O_2 \text{ (r4)}$$

$$I + HCO \rightleftarrows HI + CO \text{ (r5)}$$

$$I + H + M \rightleftarrows HI + M \text{ (r6)}$$

I regeneration:

$$HI + H \rightleftarrows H_2 + I \text{ (r7)}$$

$$HI + OH \rightleftarrows H_2O + I \text{ (r8)}$$

$$HI + CH_3 \rightleftarrows CH_4 + I \text{ (r9)}$$

$$HI + HCO \rightleftarrows H_2CO + I \text{ (r10)}$$

The differences observed between CF_3Br and CF_3I on laminar flame speed for methane around the stoichiometric condition are due to the difference in reactivity between I and Br. One of the main outcomes of this study is the discrepancy observed between the model and the data on the suppressant effect of CF_3I on C_2H_4. The sensitivity analysis on $OH^{\bullet}$ did not report any sensitive reaction involving species related to CF_3I and confirmed the experimental observation on the lack of effect of CF_3I on τ_{ign} at high temperature. At lower temperature (1340 K), the inhibiting reactions r2, r3, r4, r5, and r7 are within the 25 most-sensitive reactions. These reactions are common with the other hydrocarbons for the most part, and this list of important reactions therefore indicates that the reaction rate of most of these reactions would need to be revisited to improve the predictions.

5. Conclusion

During this study, the effect of CF_3I addition on the ignition delay times and laminar flame speeds of methane, ethylene, and propane was studied experimentally for the first time. Overall, the effects on the ignition delay time were found to be fuel dependent: a decrease in τ_{ign} was observed with methane, whereas an increase in τ_{ign} was observed at low temperature with C_2H_4 and, to a lesser extent, with C_3H_8. Flame speed measurements allow assessing the suppressant effect of CF_3I. A significant reduction in the flame speed was observed for all three fuels. The comparison, when possible, between of the effects of CF_3I and CF_3Br showed a greater suppressant effect of the latter in the present conditions. The comparison with detailed kinetics models showed good agreement with the results with CH_4 and C_3H_8. However, the effect of CF_3I on C_2H_4 ignition was poorly predicted. The chemical analysis showed that the interactions between the radical I and the radical and molecules from the hydrocarbon sub-mechanism would need to be revisited.

Acknowledgments

Financial support was provided by the Mary Kay O'Connor Process Safety Center at the Artie McFerrin Department of Chemical Engineering, Texas A&M University for the TAMU effort and by CNRS-France for the work performed at ICARE, CNRS-INSIS Orléans.

Appendix A. Supplementary data

Supplementary data associated with this article can be found, in the online version, at http://dx.doi.org/10.1016/j.proci.2014.05.096.

References

[1] T. Noto, V. Babushok, A. Hamins, W. Tsang, *Combust. Flame* 112 (1998) 147–160.
[2] J. Douglas Mather, R.E. Tapscott, in: Richard G. Gann (Ed.), *Advanced Technology for Fire Suppression in Aircraft – The Final Report of the Next Generation Fire Suppression Technology Program*, NIST Special Publication 1069, 2007, p. 611.
[3] G.T. Linteris, D.R. Burgess, F. Takahashi, V.R. Katta, H.K. Chelliah, O. Meier, *Combust. Flame* 159 (2012) 1016–1025.
[4] Y. Saso, *Proc. Combust. Inst.* 29 (2002) 337–344.
[5] C.H. Osorio, A.J. Vissotski, E.L. Petersen, M.S. Mannan, *Combust. Flame* 160 (2013) 1044–1059.
[6] V. Babushok, W. Tsang, *Combust. Flame* 123 (2000) 488–506.
[7] C. Luo, B.Z. Dlugogorski, E.M. Kennedy, *Fire Technol.* 44 (2008) 221–237.
[8] C.K. Westbrook, *Combust. Sci. Technol.* 34 (1983) 201–225.
[9] V. Babushok, T. Noto, D. Burgess, A. Hamins, W. Tsang, *Combust. Flame* 107 (1996) 351–367.
[10] T. Noto, V. Babushok, D.R. Burgess Jr., A. Hamins, W. Tsang, A. Miziolek, *Proc. Combust. Inst.* 26 (1996) 1377–1383.
[11] K.C. Smyth, D.A. Everest, *Proc. Combust. Inst.* 26 (1996) 1385–1393.
[12] O. Sanogo, J.L. Delfau, R. Akrich, C. Vovelle, *J. Chim. Phys. Phys.-Chim. Biol.* 93 (1996) 1939–1957.
[13] C.J. Aul, W.K. Metcalfe, S.M. Burke, H.J. Curran, E.L. Petersen, *Combust. Flame* 160 (2013) 1153–1167.
[14] E.L. Petersen, M.J.A. Rickard, M.W. Crofton, E.D. Abbey, M.J. Traum, D.M. Kalitan, *Meas. Sci. Technol.* 16 (2005) 1716–1729.
[15] T. Dubois, N. Chaumeix, C. Paillard, *Energy Fuels* 23 (2009) 2453–2466.

[16] P.D. Ronney, G.I. Sivashinsky, *SIAM J. Appl. Math.* 49 (1989) 1029–1046.

[17] COSILAB, *The Combustion Simulation Laboratory, Version 3.3.2.*, Rotexo GmbH & Co. KG, Haan, Germany, 2009, <http://www.SoftPredict.com>.

[18] W.K. Metcalfe, S.M. Burke, S.S. Ahmed, H.J. Curran, *Int. J. Chem. Kinet.* 45 (2013) 638–675.

Please cite this article in press as: O. Mathieu et al., *Proc. Combust. Inst.* (2014), http://dx.doi.org/10.1016/j.proci.2014.05.096